PHILIPS TECHNICAL REVIEW

VOLUME 30, 1969, No. 3

A step-and-repeat camera for making photomasks for integrated circuits

F. T. Klostermann

In the current technique for making monolithic integrated circuits a large number of identical electronic circuits, each consisting of a number of circuit elements, are formed upon a silicon wafer perhaps 50 mm in diameter. This technique has only been made possible by the most extensive refinements in mechanical and chemical processing. A particularly important part is played by the photographic step-and-repeat process which has to meet some exceptionally difficult accuracy requirements. The cameras which Philips have developed for this process can produce photomasks with an accuracy of 0.2 μm or better.

Introduction: technology of monolithic integrated circuits

Monolithic integrated circuits consist of very small but complicated structures, with even smaller detail and tolerances, which are formed in a silicon crystal. The desired configurations are obtained by using a refined photographic technique. The basic steps in the process are shown in *fig. 1* [1]. A coating of photosensitive lacquer (photoresist) is deposited on a wafer of silicon oxidized at its surface. A microphotographic negative, the photomask, is placed on the wafer and the coating of photoresist is exposed to the light of a mercury lamp. The exposed areas of photoresist are dissolved in a liquid developer (with another type of photoresist it is the unexposed parts which are dissolved). At the places no longer covered by photoresist the layer of SiO_2 can be dissolved in a selective etching bath, and the remaining photoresist is then removed. This photo-etching process is followed by a diffusion process which gives the desired doping to the areas of silicon from which the oxide has been removed by etching; a new layer of SiO_2 is then formed. These processes, from the application of the photoresist to the formation of a new layer of SiO_2, have to be repeated a number of times with different masks and different types of diffusion, as

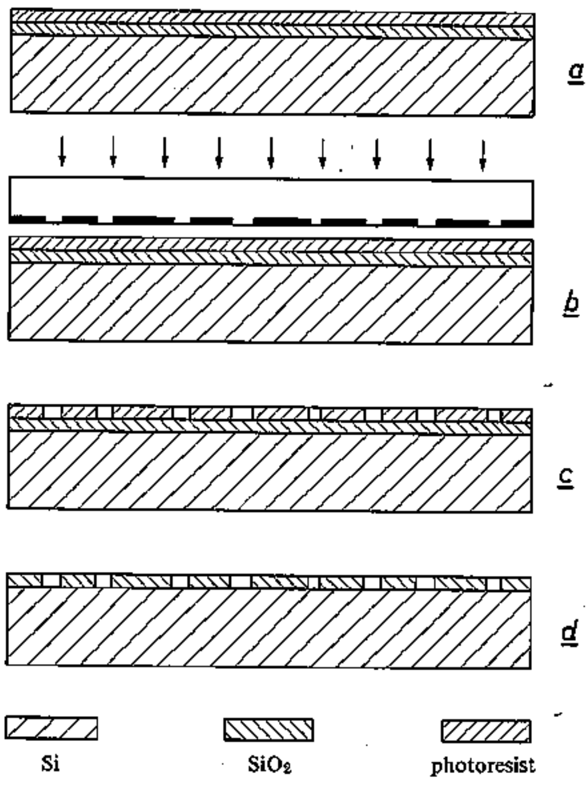

Fig. 1. Photographic process in the manufacture of integrated circuits.
a) Silicon substrate with SiO_2 layer and coating of photoresist.
b) Exposure in contact with a photomask.
c) The exposed parts of the photoresist are dissolved.
d) The SiO_2 layer is etched away at the places where the photoresist has been dissolved, then the remaining photoresist is dissolved.

Ir. F. T. Klostermann is with Philips Research Laboratories, Eindhoven.

[1] For a more detailed description see A. Schmitz, Solid circuits, Philips tech. Rev. 27, 192-199, 1966.

required for the circuit to be produced. Finally, a "wiring" of deposited aluminium is formed by using similar processes with what is called the aluminium or wiring mask.

In this article we shall not go into the electrical characteristics required of the circuits or the silicon-doping processes involved, but we shall look instead at the mechanics of the photographic process, with particular attention to the manufacture of the photomasks used in this process.

details of this size on the photoresist on the silicon wafer (fig. 1*b*).

b) In the succession of processes that are applied in making an integrated circuit, *windows* have to be made at each step in newly formed layers of SiO_2. These windows should match each other very closely, often with tolerances of not more than say $\pm \frac{1}{2}$ μm. *Fig. 2* shows a circuit together with the set of photomask patterns (in this case five) which were used successively in making it.

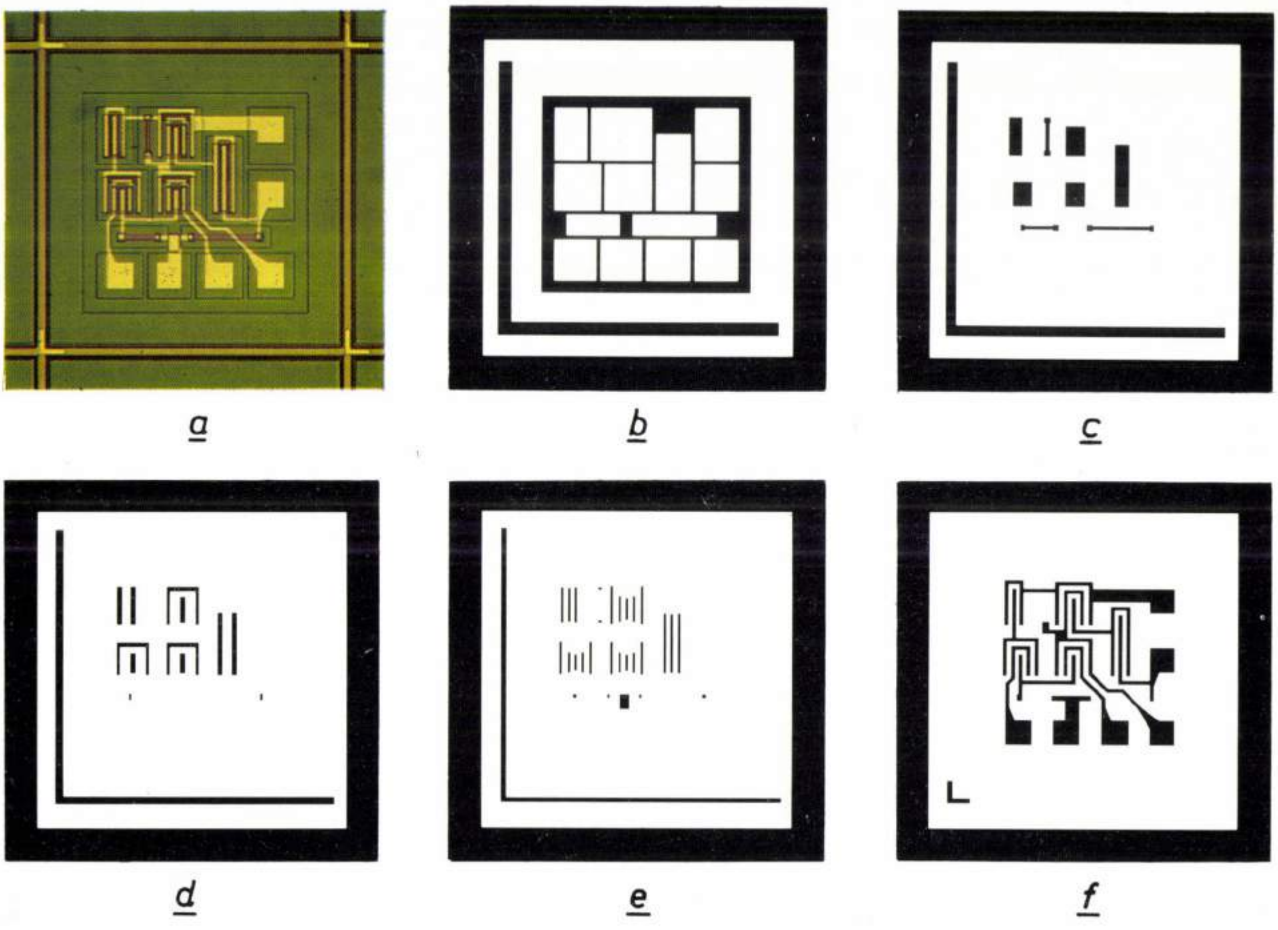

Fig. 2. *a*) An integrated circuit enlarged about 40×. *b-f*) Patterns for the photomasks used to produce circuit (*a*).

Accuracy requirements for photomasks

The requirements which the photomasks have to meet are determined by three special features of the technique employed:

a) The dimensions of elements in an integrated circuit or in a transistor for high frequencies have to be extremely small (down to 1 μm in extreme cases). The patterns on the photomask have to be sharp enough to give accurate and reliable copying of

c) A large number of circuits are formed simultaneously on a single silicon wafer. Each of the photomasks therefore has to be made up from a large number of regularly spaced identical patterns; there are 100 to 10 000 patterns on a mask. *Fig. 3* shows a multiple photomask of this type for one of the mask patterns shown in fig. 2 (the wiring mask).

Each of the multiple photomasks in a set has to be copied in contact with the coating of photoresist on the silicon wafer in such a way that *all* the successive patterns register with each other over the *entire* surface within the $\pm \frac{1}{2}$ μm tolerance. This is only possible if the mask patterns are very accurately located in the same way in each of the photomasks. In placing the successive photomasks on the silicon wafer, errors in positioning are unavoidable and also contribute to the final error in registration. The error in the position of any one pattern in the multiple mask must therefore be only part of the total tolerance, say $\pm \frac{1}{4}$ μm. This should be compared with the size of the complete mask, which is 50 000 μm.

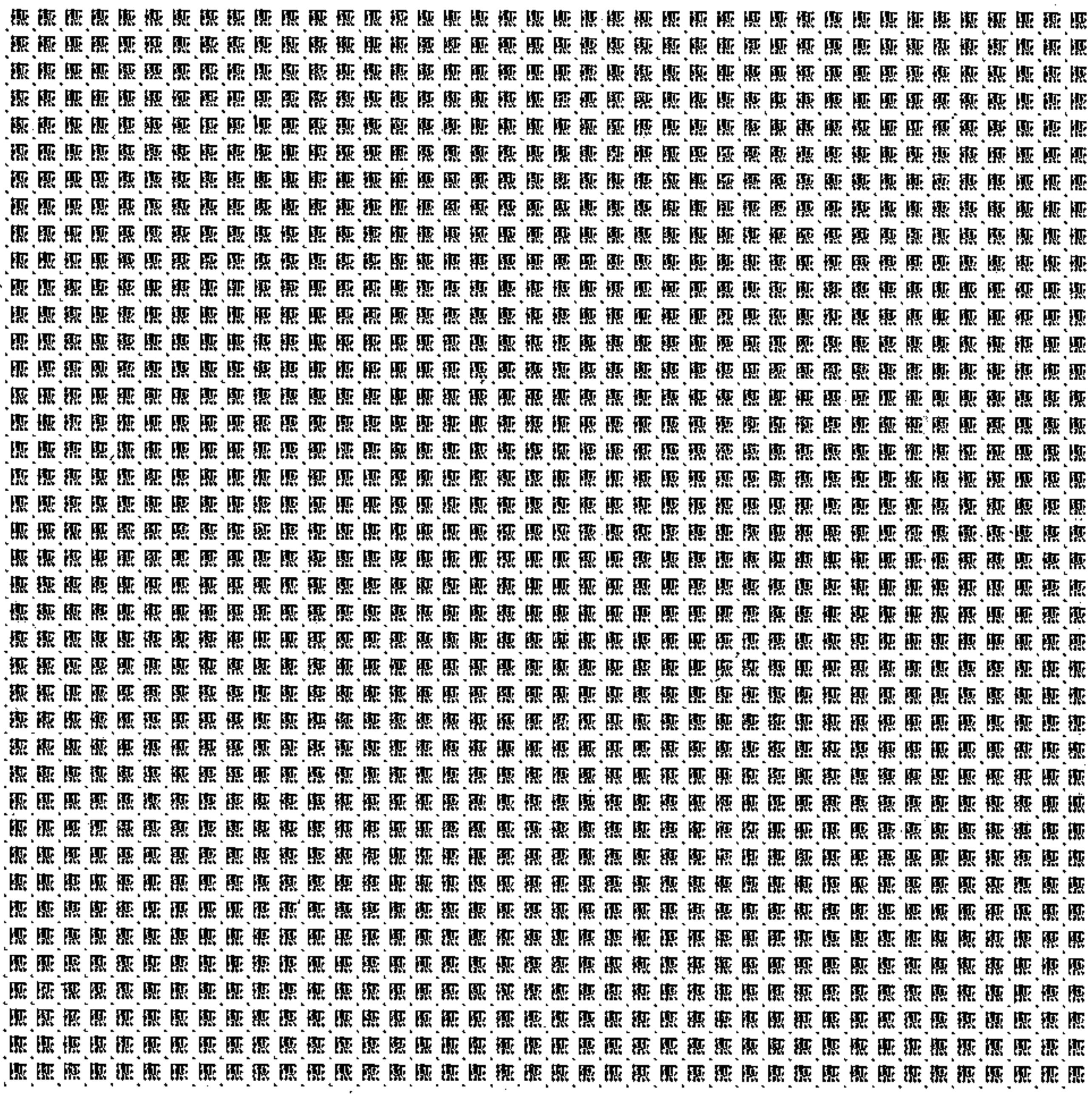

Fig. 3. Multiple photomask, enlarged 3×, of the pattern shown in fig. 2*f* ("aluminium" mask used to apply the wiring).

Limitations imposed by image quality

The degree of sharpness of the pattern which can be achieved in the microphotographic negative is limited by aberrations and diffraction in the optical image, by light scattering during exposure, and by chemical diffusion during the development of the photographic plate. If visible light and a very fine-grained silver-halide plate (Lippmann plate) are used, lines 1 μm wide can be obtained with just sufficient sharpness.

Ultra-violet light has the advantage that it suffers less diffraction than visible light. The Rayleigh scattering of light in Lippmann plates, however, increases with decreasing wavelength and with blue or ultra-violet light less sharp photographic negatives are obtained than with green light [2]. If the pattern is obtained with ultra-violet light directed at a non-scatter or reduced-scatter photographic material (such as a photoresist coating [3] or PD material [4]), lines of width less than 1 μm can be obtained which are sharp enough for practical application. In this case the limit is probably somewhere near 0.5 μm.

Much sharper images can be obtained with the aid of electron optics. Experiments using electron beam techniques have yielded particularly good results [5]. For example, conductor patterns have been produced whose line width was less than 0.1 μm. A limitation with electron beam techniques is that details in a negative which are too fine to be obtained with light optics cannot — for this very reason — be reproduced satisfactorily in the light-optical copying process mentioned above (fig. 1*b*). This makes it necessary to work without a negative and to expose each silicon wafer using the electron-optical equipment. The method is consequently very expensive, especially since the image field in which very good image quality is obtained is no larger than a few square millimetres, so that each silicon wafer has to be exposed in a great many places in turn. However, this method has other advantages besides the improved sharpness of image, so that further developments along these lines seem likely.

Making masks photographically by the step-and-repeat technique

One of the fundamental problems of the technology we have described is that of making the multiple photomasks to the required accuracy. In one ingenious method a pinhole array camera with a large number of uniformly spaced holes is used, giving a reduced image of the same mask pattern behind each hole [6]. Unfortunately, the image quality which can be obtained is not good enough. In the "fly's-eye" camera proposed by IBM each hole is replaced by a simple moulded plastic lens. The image quality achieved by this means is acceptable for certain applications [7].

However, the most important and almost universally employed method of producing photomasks is the step-and-repeat technique. With this technique the multiple photomask is obtained by optically recording the mask pattern not simultaneously but *successively*, on a reduced scale, at a number of positions on a photographic plate. The chief advantage of this method is that the "step-and-repeat camera" used for this process can be provided with a very good optical system whose image field has been matched to the size of the mask patterns. Achieving the very high register accuracy which is required for the multiple photomasks of a set now depends on the accuracy of the displacement system of the step-and-repeat camera.

Before discussing this matter in further detail let us briefly mention some important features of the step-and-repeat technique [8].

To begin with, mask patterns are usually prepared at a scale of say 200 : 1, with the aid of a numerically controlled drawing-machine [9]. These patterns are then reduced in two stages: the first reduction, which could typically be 10×, provides the object plates for the step-and-repeat camera, and the second reduction, of 20×, is carried out by the step-and-repeat camera itself [10]. In this second reduction, the plates used are of the silver-halide type used in microphotography, like the Kodak High Resolution plate. The plate can be exposed "in motion" in the step-and-repeat camera by using a xenon flash lamp; the photographic plate moves uniformly in its own plane and the flash lamp is fired whenever a position is reached at which an image of the pattern must appear. This position is determined by means of a measuring system. The duration of the flash from the lamp can be so short (e.g. 10 μs) that the movement causes no loss of sharpness at quite practical rates of advance of the photographic plate (e.g. 1 mm/s). The operation of a step-and-repeat camera with "in motion" exposure is shown schematically in *fig. 4*. The carriage S carrying the photographic plate moves uniformly on a slideway and this permits a row of very accurately located patterns to be obtained relatively easily and quickly. The starting point of each successive row has to be set each time (manually or by servo) by displacing a second carriage which carries the projection system and moves at right angles to S.

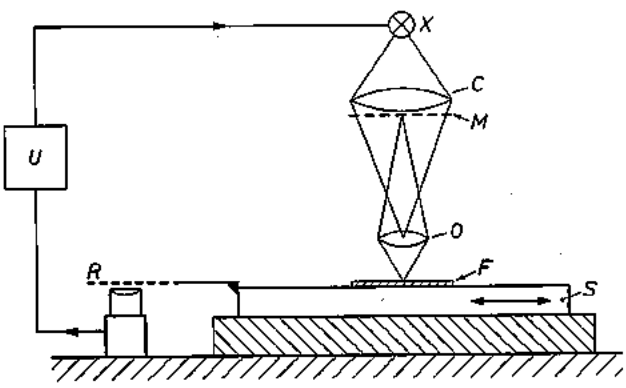

Fig. 4. Step-and-repeat camera with "in motion" exposure for generating a multiple photomask. M object plate with a mask pattern, positioned in a projection system with xenon flash lamp X, condenser lens C and objective O. The photographic plate F is on a carriage S which moves at uniform speed. The measuring system using a grating R determines the distance covered and gives this information to the control and supply circuit U which fires the flash lamp at the correct instants. The projection system is placed on a second carriage, similar to S and moving at right angles to S, whose displacement is determined with a second measuring system.

To increase the production capacity a *multiple* step-and-repeat camera (a "multi-barrel camera") is generally employed. The principle shown diagrammatically in fig. 4 remains unchanged and no drastic modifications need be made to the slide systems, the measuring system or the control circuit. A number of projection systems — six, for example — rigidly fastened to each other, and with their flash lamps fired by the same pulse, are placed side by side on one carriage and six photographic plates are fitted to the other, which moves at right angles to the first (*fig. 5*). Six different object

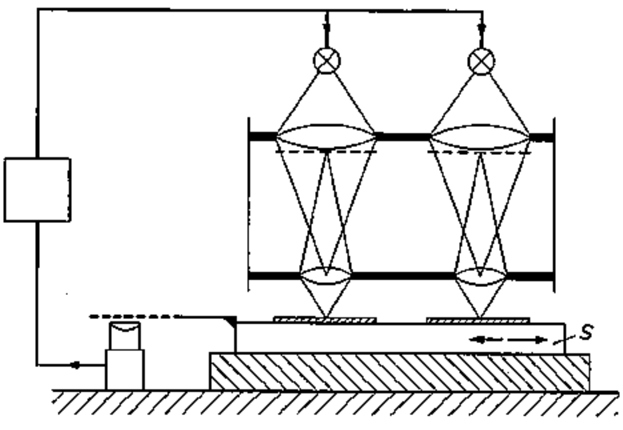

Fig. 5. Multiple step-and-repeat camera with "in motion" exposure. Two rows of three photographic plates are mounted on carriage *S*, each plate being exposed by its own projection system. The two rows of three projection systems are themselves mounted on a second carriage which moves at right angles to *S*.

plates, each showing one of the mask patterns required for a set of photomasks, are inserted in the projection systems. In this way all the photomasks required for an integrated circuit (usually not more than six to ten) can be prepared in one or two runs.

With the multi-barrel camera, it is essential that both simultaneously and successively made photomasks should match each other exactly. The most critical factors here are:

a) The accuracy of the slide systems.
b) The accuracy of the measuring system.
c) The positioning of the object plates.
d) The maintenance of focus and the correct reduction factors.
e) Temperature control.

An equipment that satisfies current (and even more stringent) requirements in all these respects has been developed in our Laboratories: under the least favourable conditions of use it gives a total error from all these sources which is no greater than $\pm$ 0.2 µm. The various critical factors will be considered in the discussion of the equipment which follows.

The Philips step-and-repeat camera

The slide systems

The ultimate accuracy of the photomasks depends to a very large extent on the slide systems of the step-and-repeat camera. The two most important requirements which the slide systems must satisfy are that the random lateral deviations (perpendicular to the direction of travel) must be extremely small and that rotation about the optical axes of the camera must be kept to an absolute minimum. Lateral deviations give rise to errors in photomasks which are made successively. Rotation of the carriages about the optical axes causes errors in photomasks that are made simultaneously by the different projection systems. If the distance between the optical axes is d and there is a rotation of $\Delta\alpha$, relative errors of $d\Delta\alpha$ are introduced.

A slide system with hydrostatic bearings which is ideally suited for the step-and-repeat technique has been developed (for other purposes) in these Laboratories by De Gast [11]. The design of a slide system of this

[2] G. W. W. Stevens, Microphotography; photography and photofabrication at extreme resolution, Chapman and Hall, London 1968, p. 27.

[3] H. J. Schuetze and K. E. Hennings, Large-area masking with patterns of micron and submicron element size, Semicond. Prod. Solid State Technol. 9, No. 7, 31-35, 1966.

[4] H. Jonker, C. J. Dippel, H. J. Houtman, C. J. G. F. Janssen and L. K. H. van Beek, Physical development recording systems, I. General survey and photochemical principles, Phot. Sci. Engng. 13, 1-8, 1969 (No. 1); parts II, III, IV, V to appear shortly.

[5] T. H. P. Chang and W. C. Nixon, Electron beam formation of 800 Å wide aluminium lines, J. sci. Instr. 44, 231-234, 1967.

[6] J. J. Murray and R. E. Maurer, Arrays of microphotographs for microelectronic components, Semicond. Prod. 5, No. 2, 30-32, 1962.
P. A. Newman and V. E. Rible, Pinhole array camera for integrated circuits, Appl. Optics 5, 1225-1228, 1966.

[7] W. E. Rudge, W. E. Harding and W. E. Mutter, Fly's-eye lens technique for generating semiconductor device fabrication masks, IBM J. Res. Devel. 7, 146-150, 1963. — An interesting new method that promises high image quality is the holographic method of simultaneous image multiplication recently proposed by G. Groh of the Philips laboratory at Hamburg (Appl. Optics 7, 1643-1644, 1968), now being further investigated there.

[8] A. J. O'Malley, The ABC's of photomasking, Semicond. Prod. Solid State Technol. 7, No. 11, 27-32, 1964.

[9] R. Ch. van Ommering and G. C. M. Schoenaker, The "COBRA", a small digital computer for numerical control of machine tools, Philips tech. Rev. 27, 285-297, 1966. A recent further development of this work is described by C. Niessen and H. E. J. Wulms, Automatic drawing of masks for integrated circuits, Philips tech. Rev. 30, 29-34, 1969.

[10] More direct methods for the first step have been developed and further development is expected: in these methods the object plates for the step-and-repeat camera are obtained directly by numerically controlled exposure of the photographic plate. See for example: H. Freitag, Generating IC masks automatically, Electronics 40, No. 18, 88-92, 1967.

[11] J. G. C. de Gast, A new type of controlled restrictor (M.D.R.) for double film hydrostatic bearings and its application to high-precision machine tools; published in Advances in machine tool design and research 1966 (Proc. 7th Int. M.T.D.R. Conf., Univ. Birmingham), Pergamon Press, Oxford 1967, pp. 273-298.
See also an article on a precision lathe, to appear shortly in this journal.

type is shown in *fig. 6*. The hydrostatic bearings are situated at H_1, H_2 and H_3. Oil delivered under high pressure (20 to 40 bars) by an external pump system passes first through hydraulic restrictors, with resistances R_a and R_b and then through the restrictors R_a' and R_b' formed by the narrow bearing gap (about 30 μm). This gives pressures between R_a and R_a', and also between R_b and R_b', which depend on the ratio of these resistances. A downward force on the carriage causes the gap height and hence also the intermediate pressures to change, so that a new equilibrium can be found. The slide systems designed by De Gast differ from other systems with hydrostatic bearings in that the high hydrostatic forces (approximately 10^4 newtons) are very evenly balanced. When a carriage moves, changes occur in the forces acting on the slideway. Small unavoidable asymmetries in the elastic deformation of the slideway then adversely affect the accuracy of travel. In our case however such forces are balanced, and because of this there is hardly any elastic deformation even with a carriage and slideway of relatively light construction.

The slideway for each of the two slide systems consists of three steel bars fastened to a 160 mm thick granite (diabase) slab with retaining bolts (fig. 6). The granite slab is flat to within 3 μm over the whole of its upper surface (400×600 mm). The design shown has been chosen because it enables the tendency of the carriage to rotate about the optical axes (the z-axis in fig. 6) to be effectively suppressed. In fact, any rotation about the z-axis would be caused by the guide surfaces of the bearings H_1, i.e. the opposing surfaces of bars B_2 and B_3. The average deviation of these surfaces from the straight is measured while the bars are being mounted. Any deviations measured can then be corrected by making small elastic deformations in the bars B_2 and B_3 and the corrected arrangement is made permanent with the aid of the retaining bolts.

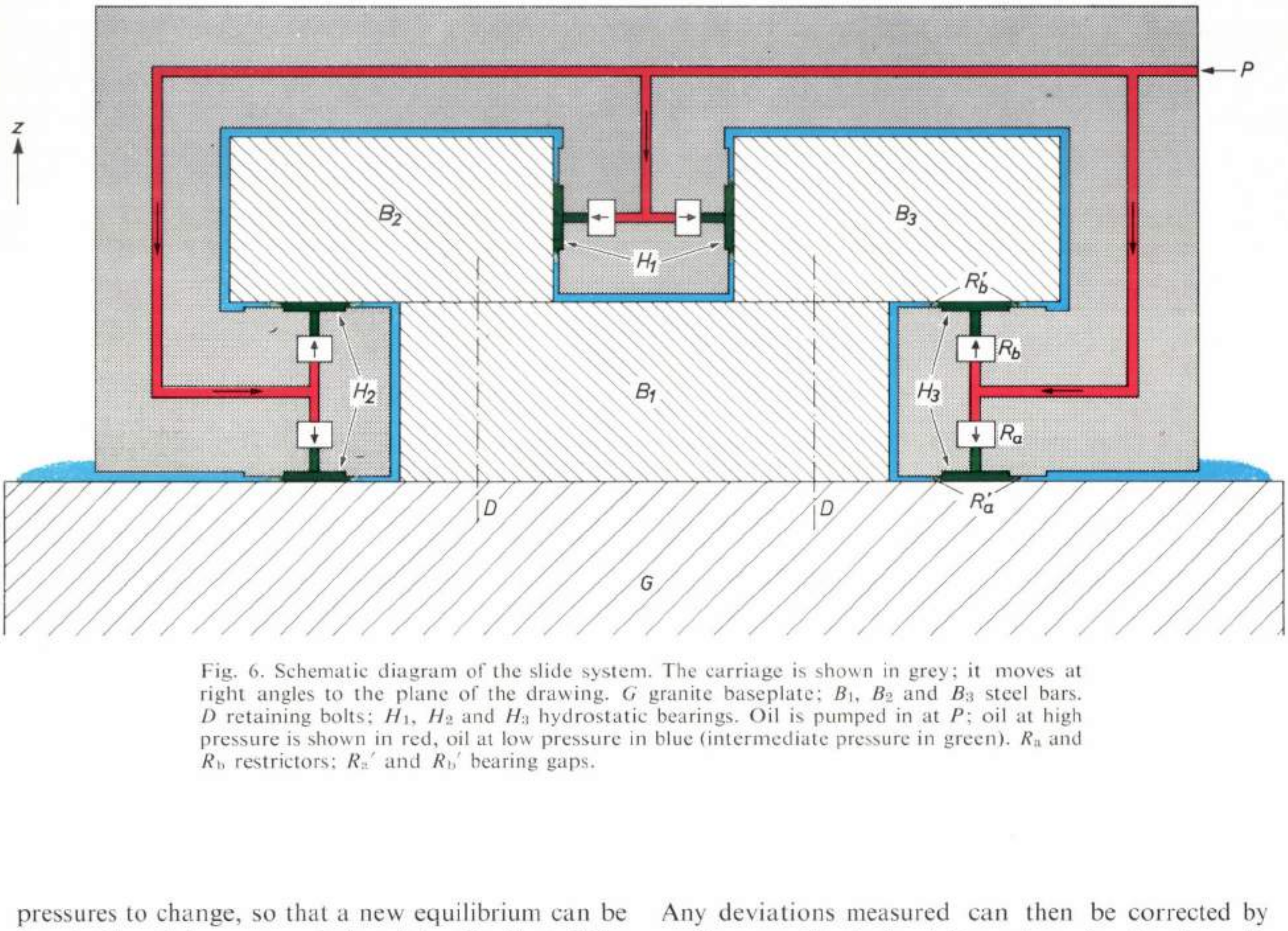

Fig. 6. Schematic diagram of the slide system. The carriage is shown in grey; it moves at right angles to the plane of the drawing. G granite baseplate; B_1, B_2 and B_3 steel bars. D retaining bolts; H_1, H_2 and H_3 hydrostatic bearings. Oil is pumped in at P; oil at high pressure is shown in red, oil at low pressure in blue (intermediate pressure in green). R_a and R_b restrictors; R_a' and R_b' bearing gaps.

The reproducibility of the paths traced out by these carriages was found by measuring the capacitance between a small metal disc mounted on the moving carriage and a fixed metal bar that had been very accurately lapped. A typical result is shown in *fig. 7*. The lateral deviations of the carriage do not exceed ± 0.03 μm.

The rotation of a carriage about the z-axis while it moved horizontally was measured with the aid of a photoelectric autocollimator telescope (measuring

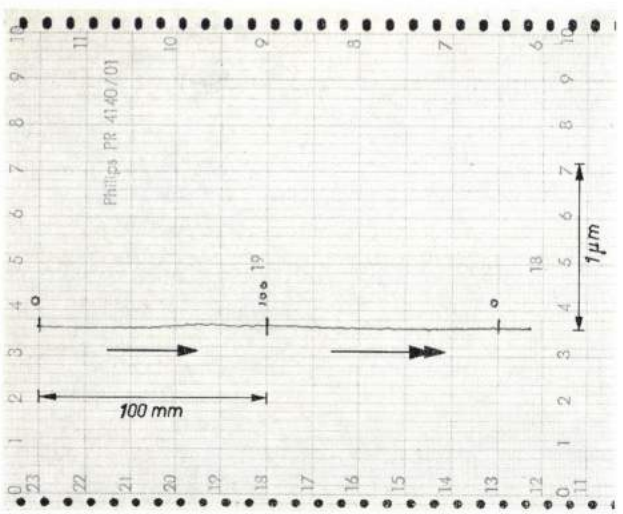

Fig. 7. Trace showing lateral deviations from the correct path of a carriage with hydrostatic bearings. The carriage has been moved 100 mm and back. The deviations are smaller than $\pm$ 0.03 mm.

accuracy 0.05 of a second of arc). A typical result is shown in *fig. 8*. The rotation about the z-axis for a travel of 50 mm does not exceed $\Delta\alpha = \pm 0.1'' = \pm 5\times10^{-7}$ rad. This has to be substituted in the formula $d\Delta\alpha$ for the resultant error. The distance required between adjacent optical axes of a multiple step-and-repeat camera depends chiefly on the size of the photomasks required. We have chosen 60 mm for this distance in one case and 80 mm in others. The largest distance, d, in our system is therefore 160 mm.

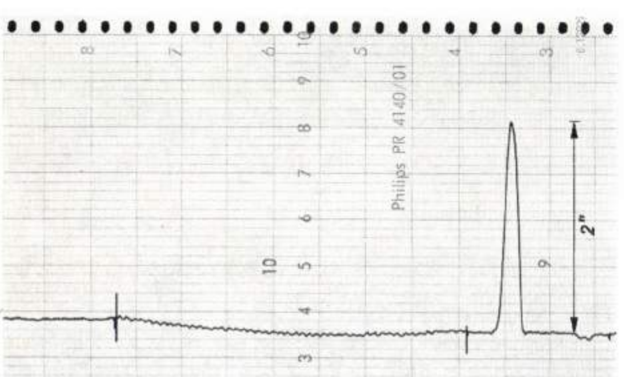

Fig. 8. Trace showing the rotation about a vertical axis of a carriage with hydrostatic bearings. Carriage movement 47 mm. Rotations are smaller than $\pm$ 0.1 second of arc. This trace was made after the slide system had been used nearly every day for 18 months.

The magnitude of the worst-case error introduced by the rotation of *both* carriages is therefore:

$$\Delta x = \pm\ 2\times16\times10^4\times5\times10^{-7} = \pm\ 0.16\ \mu\text{m}.$$

Fig. 9 shows the slide system for the six-barrel step-and-repeat camera before mounting. The carriage on which the six photographic plates are mounted can be seen at the front; the carriage at the back carries the holder for the six projection systems and moves at right angles to the first carriage. The two slide systems are mounted independently of each other on the granite slab. The dimensions of the clamping surface of each

Fig. 9. The slide systems of a six-barrel step-and-repeat camera. The carriage on which the photographic plates are mounted can be seen at the front, and the carriage at the back carries the projection systems on an arm, here already fitted.

slideway are 200×180 mm. The photograph in *fig. 10* shows the complete equipment, i.e. the actual step-and-repeat camera, and the ancillary electronic equipment which controls the movements of the carriages, the firing of the flash lamps, etc.

The measuring system

Indirect methods of measuring carriage travel, such as the combination of an angle-measuring system and a lead-screw, are much used in engineering workshops. However, the indirect methods are not very suitable in our case, since such methods are barely capable of the high linear measuring accuracy required. For the accuracy that we require, a direct measurement of displacement, by optical means, is by far the most suitable. Two such systems have been developed in these Laboratories by De Lang and others; both systems can be considered for the step-and-repeat camera. One is a grating measurement system, and the other a laser-interferometer system [12]. Of the two, the former depends on the barometric pressure, and it introduces a measuring unit that is basically foreign to the metric system. The small systematic errors that can occur with a measuring grating (perhaps ± 0.2 µm) are no disadvantage in our case where we are chiefly concerned with the *relative* registration of the photomasks.

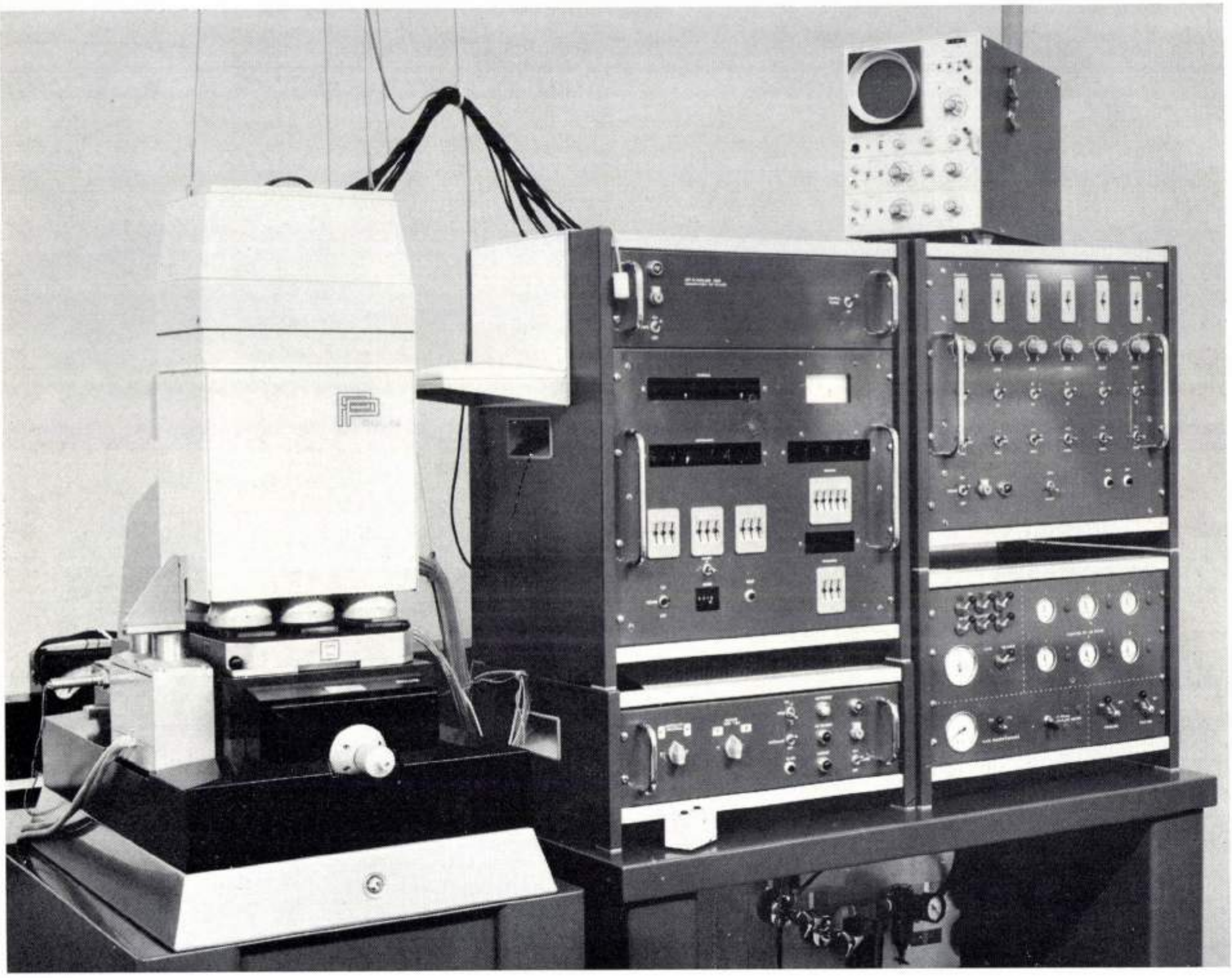

Fig. 10. The complete six-barrel step-and-repeat camera. The panels on the right contain the electronic control and supply circuits, the reducing valves for pressurizing the air bearings, and other accessories.

appears more suitable for the step-and-repeat technique because the thermal expansion coefficient of the measuring grating can be matched to that of the glass photographic plate by appropriate choice of the material of the grating. The actual temperature level of the step-and-repeat camera is then far less critical, which is quite the reverse of the situation with a laser interferometer, whose thermal expansion coefficient is some 10 times smaller than that of most types of glass. Moreover, measurement with a laser interferometer

For a detailed description of the grating measurement system, which is being used with very good results in our step-and-repeat camera, the reader is referred to the publication already noted under [12]. A detail which should be mentioned here is that measurement with this system makes use of a mirror vibrating at a frequency f. When the system is used dynamically, as when flash lamps are fired during the uniform movement of the carriage, the frequency f and the velocity v of the carriage together impose a limit on the repetition accuracy that can be obtained by the measurement. This is because the uncertainty Δt of the instant of firing is $\pm 1/2f$, and the uncertainty in the location of the images is therefore $\Delta x = \Delta t \times v = \pm v/2f$. With $v = 1$ mm/s and $f = 4$ kHz, we obtain $\Delta x = \pm 1/8$ μm.

Fig. 11 is a close-up view of the measuring head and measuring grating assemblies in the six-barrel step-and-repeat camera. The measuring heads, which are firmly fixed to the granite base plate, read off the gratings from below.

Fig. 11. The measuring system. The measuring head and the grating on the left are for the carriage on which the photographic plates are mounted; the measuring head and grating on the right are for the carriage carrying the projection systems.

Positioning of the object plates

The patterns $a_1, b_1, c_1 \ldots$ of a set of multiple photomasks can only yield accurately registering prints if they all make the same angle with the directions of travel in the step-and-repeat process. This condition can be satisfied by positioning the object plates for patterns $a_1, b_1, c_1 \ldots$ in the projection system very accurately to the same angle. Sometimes a pattern $a_1, b_1, c_1 \ldots$ has to be left out at certain positions on the photomask, and another pattern $a_2, b_2, c_2 \ldots$ has to be put in at these positions (for example for putting in special test components). If this is the case a second condition is added: the object plates for patterns $a_1, b_1, c_1 \ldots$ and $a_2, b_2, c_2 \ldots$ must also be positioned very accurately to the same coordinates.

This positioning adjustment can be performed by the following simple and reliable method. Each object plate has two optical fiducial marks and the top plate of the projection column (the housing of the projection systems) on which the object plates have to be successively placed, has "enclosing" lines which fit round the marks (*fig. 12*). The two marks are 25 mm apart. A double

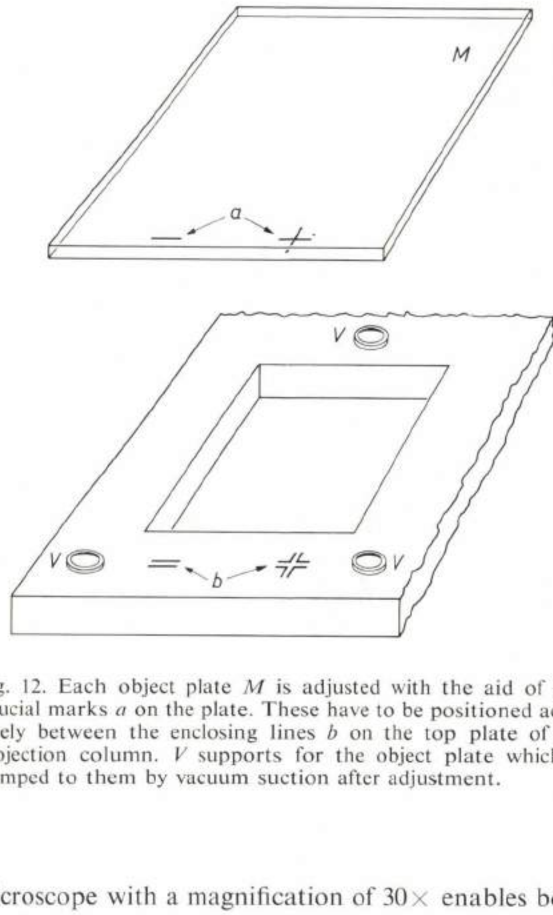

Fig. 12. Each object plate M is adjusted with the aid of two fiducial marks a on the plate. These have to be positioned accurately between the enclosing lines b on the top plate of the projection column. V supports for the object plate which is clamped to them by vacuum suction after adjustment.

microscope with a magnification of 30× enables both marks to be observed simultaneously (*fig. 13*). Firmly attached to the microscope is an x-y-α micromanipulator which can be used to move the object plate so that the marks fit between the enclosing lines. The combined adjustment microscope and micromanipulator can be positioned over each of the projection systems by means of a subsidiary slide system and held there temporarily by pistons powered with compressed air.

The positioning of a black line centrally between two black enclosing lines is in fact checked visually by comparing the light intensity of the strips left between

[12] Both systems will shortly be described in this journal.

the lines; the eye can detect an extremely small asymmetry between the two intensities. With a suitable configuration of the enclosing lines [13] it is possible in this way to detect a deviation as small as $\Delta x = \Delta y = \pm 0.3$ μm when the magnification is only 30×. A setting accuracy of ± 1 μm is easily and quickly ensured with the micromanipulator.

One of the reasons why this method is so reliable is that the accuracy of the subsidiary slide system does not affect the result.

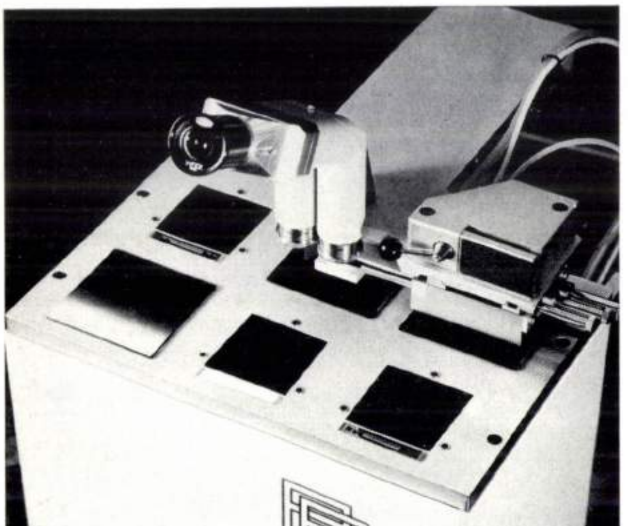

Fig. 13. The adjustment microscope with the x-y-α micromanipulator to the right of it.

Focusing and reduction factor

Each of the six optical systems of a step-and-repeat camera has to project an image of its object plate on each of the successive desired positions of the appropriate photographic plate. In this operation the optical system must remain accurately focused on the surface of that plate. Any defocusing affects not only the sharpness but also the size of the image.

Contrary to what might be expected, the effect on image size is in some cases more serious than the loss of sharpness. This should be clear from the following estimate of the tolerances of the two effects. To obtain good image quality in microphotography a fairly large numerical aperture value N is necessary, e.g. $N = 0.2$ to 0.4. The depth of focus, given by $\Delta b = \pm 0.6\,\lambda/N^2$, and hence the amount of defocusing allowed if adequate image sharpness is to be retained, is consequently very small. Using the above values for N and a wavelength of $\lambda = 0.5$ μm we find $(\Delta b)_{\max} = \pm 8$ to 2 μm. On the other hand, a variation Δb in the image distance b causes an image point at a distance r from the optical axis to be shifted by Δr, and this variation of the image size means that projected images will be out of register. As a first approximation $\Delta r/r = \Delta b/b$. (More correctly, b should be replaced by the distance between image plane and exit pupil.) In the optical systems used in practice $b/r_{\max}$ often has a value between 10 and 20. If we assume Δr, the tolerance on r, to be $\frac{1}{8}$ or $\frac{1}{4}$ μm, we see that in some (in fact important) cases the defocusing Δb allowed giving the maximum allowable change in image size will only be about ± 2 μm. If this requirement is met, the depth-of-focus requirement given above is automatically satisfied.

The most important cause of defocusing is out-of-flatness of the photographic plate. Kodak High Resolution plates are generally used, in the versions known as "selected flat" and "ultra flat" (the "micro flat" version is not very suitable because of the thick glass). Over a length of 25 mm the guaranteed tolerance on flatness is ± 25 μm for "selected flat" plates and ± 10 μm for "ultra flat" plates. The length we are concerned with, however, is considerably larger than 25 mm, since the size of the field with mask patterns is about 50 mm in multiple photomasks for integrated circuits. Since other factors besides flatness, e.g. placing the photographic plate against stops, contribute to the total defocusing Δb, the tolerance calculated above is far exceeded even with "ultra flat" plates.

This difficulty has been overcome by continuously correcting the image distance b while the photographic plate is moving, using the local surface of the plate itself as reference level [14]. We have achieved this in our camera by mounting each objective in diaphragm springs and allowing it to rest on an air bearing over the part of the photographic plate which is to be exposed (*fig. 14*). With a supply pressure of 2 bars and a nominal gap height of 20 μm in the air bearing, the gap height varies by 1 μm per 0.1 bar change in the supply pressure. The gap height in this case can easily be kept constant within ± 1 μm. This air-bearing focusing arrangement can be seen in *fig. 15*. The photographic plates have to be brought up to the air bearings from underneath. To load the camera, the plate holder is swung out, loaded with plates, swung under the air bearings in the lowest position and automatically adjusted to the correct height by three compressed-air pistons.

Temperature control

The principle of the step-and-repeat camera is that the plate (or group of six plates) is displaced by increments — longitudinal for the continuous movement

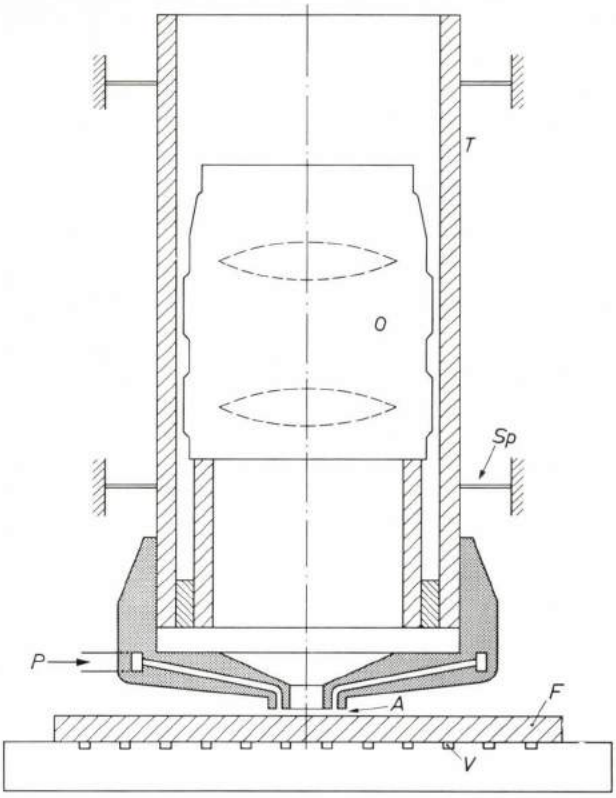

Fig. 14. To prevent defocusing due to out-of-flatness of the photographic plate, the objective mounted in tube T is mounted in diaphragm springs Sp and held by an air bearing A at an accurately constant height from the part of the photographic plate F to be exposed. The compressed air for the bearing is supplied at P. V vacuum suction plate.

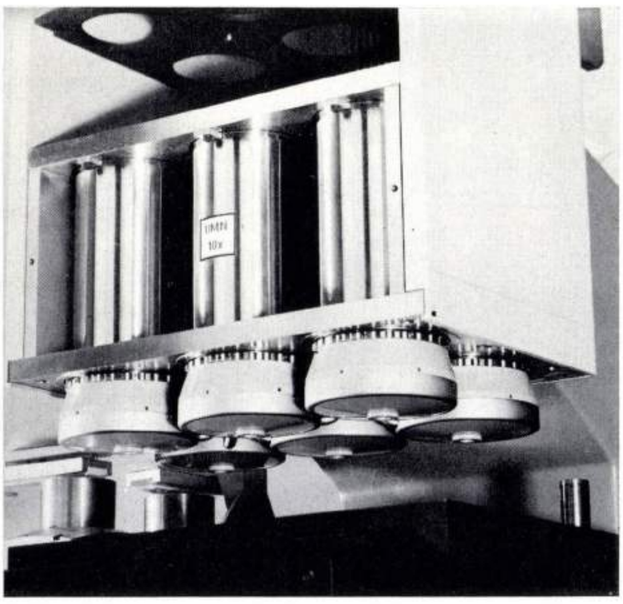

Fig. 15. Arrangement for focusing by means of air bearing. The objective tubes are mounted in diaphragm springs. The circular air bearing can be seen at the lower end of each tube.

and lateral at the start of a row of new patterns — which are accurately established with respect to the axis of the projection system. With the measurement system just described, however, the displacement produced inevitably has to be measured at a certain distance from the optical axes. Due allowance must be made for the possibility that the accuracy of location of subsequent rows of patterns is adversely affected by changes in the distance between the measuring point and the optical axis, or between the measuring point and the photographic plate; see *fig. 16*. Such changes may occur

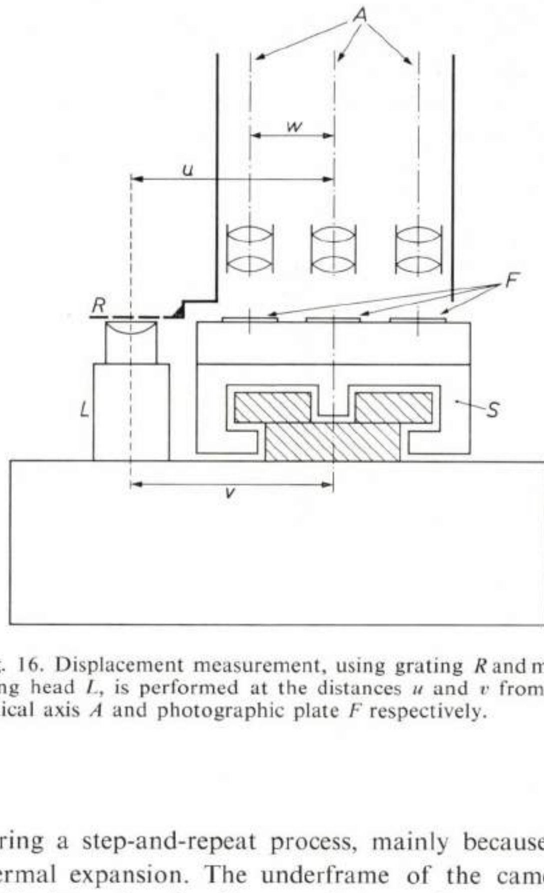

Fig. 16. Displacement measurement, using grating R and measuring head L, is performed at the distances u and v from the optical axis A and photographic plate F respectively.

during a step-and-repeat process, mainly because of thermal expansion. The underframe of the camera, which determines the distance v between the measuring head and the photographic plates, is largely made of granite; the upper part of the structure, however, which determines the distance u between the measuring grating and the optical axes, is mainly made of steel and is much more lightly constructed. The thermal expansion of the two parts thus differs greatly and

[13] P. Kissam, Optical tooling for precise manufacture and alignment, McGraw-Hill, New York 1962, pp. 116-118.

[14] A forerunner of this method is the one proposed by Bovey, for finding the distance by measuring an airflow resistance. See E. Bovey, Pneumatic gauging applied to the focusing of a microscope objective, British Scientific Instrument Research Association, Research Report No. 51, July 1954.

temperature changes during the step-and-repeat process therefore introduce errors.

Because of this situation the temperature of the oil supplied to the hydrostatic bearings is kept constant to within ± 0.05 °C and the flow of oil to the bearings is also maintained during temporary halts in the process. The temperature of the air supplied to the air bearings is controlled to within ± 0.1 °C. To bring the oil and air to the same final temperature the two controlled temperatures have to be set to different values, since the frictional heat developed in the oil restrictions makes the oil about 1 °C warmer, while the Joule-Kelvin effect cools the air in the air-bearing gap by about 0.5 °C.

One factor that helps to give good temperature control is that the camera is in much better thermal contact with the bearing oil than with the air in the room where it is installed — the temperature in this room varies by considerably more than 0.05 °C. Camera warm-up by radiant heat from the operator can be prevented by a simple radiation screen.

To eliminate as far as possible thermal expansion at the measuring head — where errors would have a particularly undesirable effect — the lamps in the measuring heads have been chosen to have a dissipation as small as possible: it is less than 0.1 W per head.

We have measured the temperatures at a number of critical points in one of our step-and-repeat cameras in normal use in a room whose temperature remained constant within ± 0.5 °C. The temperature variation ΔT at these points remained within ± 0.1 °C during a period of 1 hour. In the overall repetition error the contribution that can be expected from temperature changes is proportional to ΔT; it is also proportional to the distance w (see fig. 16) for photomasks made simultaneously and to the distance u for photomasks made successively. If $w = 80$ mm and $u = 150$ mm, the error contributions are found to be ± 0.08 μm and ± 0.15 μm respectively. This estimate only makes allowance for the contraction or expansion of structural elements. Other types of distortion, such as bending, can also occur but are not particularly significant in our design of camera.

Overall repetition accuracy

From the information given above we can draw up the following list of contributions Δx to the total repetition error.

a) Slide system.
   Lateral reproducibility errors: $\Delta x_1 = \pm\, 0.03$ μm.
   Rotation ± 0.1 second of arc; therefore, for a distance of 80 mm between adjacent optical axes: $\Delta x_2 = \pm\, 0.16$ μm.
b) Measuring system (with vibrating-mirror frequency of 4 kHz).
   For a carriage speed of 1 mm/s: $\Delta x_3 = \pm\, 0.12$ μm.
c) Thermal expansion.
   For photomasks made simultaneously: $\Delta x_4 = \pm\, 0.08$ μm.
   For photomasks made successively: $\Delta x_5 = \pm\, 0.15$ μm.

Using these data we can make an estimate of the total expected repetition error from the sum:

$$\Delta x_{\text{tot}} = \sqrt{\Sigma(\Delta x_n)^2}.$$

For photomasks made simultaneously we thus find:

$$\Delta x_{\text{tot}} = \sqrt{\Delta x_2^2 + \Delta x_4^2} = \pm\, 0.1 \ \mu\text{m},$$

and for photomasks made successively:

$$\Delta x_{\text{tot}} = \sqrt{\Delta x_1^2 + \Delta x_2^2 + \Delta x_3^2 + \Delta x_5^2} = \pm 0.25 \ \mu\text{m}.$$

How do these predictions compare with practical experience? The relative repetition error between two photomasks, whether produced simultaneously or successively, can be measured with a comparator arrangement; see *fig. 17*. The microscope M_1 with a fixed cross-wire is aligned on a particular mark in photomask F_1 by moving carriage S. The micrometer eyepiece E of the second microscope M_2 is then adjusted until the cross-wire is aligned on the corresponding mark in photomask F_2. Carriage S is now moved a relatively large distance, e.g. 30 mm, and M_1 is again aligned on a mark and the adjustable eyepiece of M_2 is adjusted on the corresponding mark. The difference between the two readings on the micro-

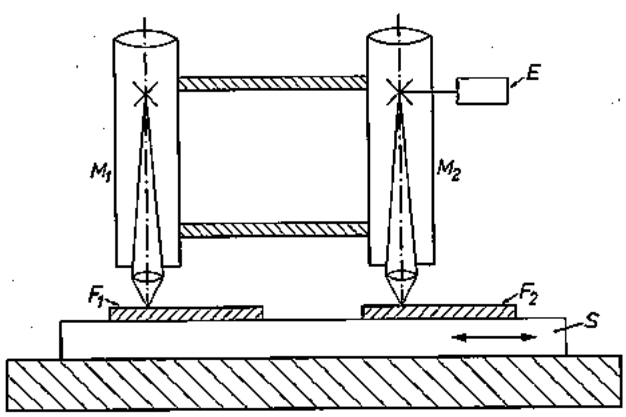

Fig. 17. Comparator arrangement for measuring the repetition error between two photomasks F_1 and F_2. These rest on a carriage S. The carriage is moved until a fixed cross-wire in microscope M_1 is aligned on a mark on F_1, and microscope M_2 is set to the corresponding mark on F_2 with the adjustable micrometer eyepiece E. The carriage is then moved through a large distance and this process is repeated.

meter eyepiece gives the relative repetition error for the two photomasks.

The main difficulty in such measurements using a comparator is that of dry friction. To overcome this difficulty, we have designed a special comparator system with hydrostatic bearings. With optimum setting marks [13] and microscopes giving a magnification of 150×, settings can be made with an accuracy of a few hundredths of a micron. We have checked this with ten successive settings of the microscope M_1 and the adjustable micrometer eyepiece E; the standard deviation calculated from the readings of E was 0.02 μm.

Using one of our six-barrel cameras we then prepared several sets of six photomasks which were given setting marks, suitable for comparator measurements. We then used the comparator to compare the distances *1-2*, *3-4*, *1-3*, *2-4*, *1-4* and *2-3*, shown in *fig. 18*, for the various photomasks. It can be seen that the greatest longitudinal or lateral displacement was 30 mm. The results of the measurement can be summarized as follows. Comparison of two photomasks made simultaneously reveals repetition errors smaller than ± 0.05 μm, while comparison of two made successively (with the same projection system) shows repetition errors smaller than ± 0.15 μm.

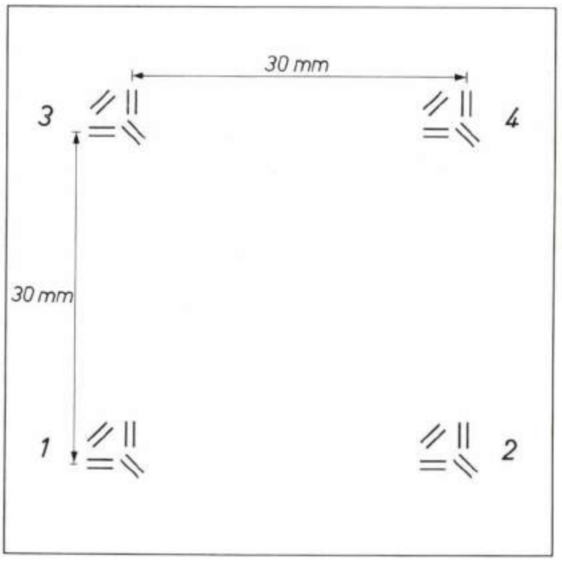

Fig. 18. Measuring points for measurements using the comparator.

It is expected that the design principles adopted in our step-and-repeat camera will ensure that the inaccuracies quoted above will not be exceeded in practice, even after a long period of use. One of the six-barrel step-and-repeat cameras has now been in service for eighteen months. The measurements reported above were made after a year of operation.

Application in integrated circuit technology

Two versions of the step-and-repeat camera have been made. The first has an optical system giving a reduction of 20× and is intended for photomasks for high-frequency transistors and for integrated circuits of relatively small dimensions. Patterns containing details with a width of 1 μm can be obtained in a field of 1.6 mm diameter with this camera. *Fig. 19* shows an example of a MOS transistor with a gate 2 μm wide, made with the aid of this camera. A 1 μm wide line is used for this gate in the photomask. By "under-etching" the SiO_2 film, which is 0.6 μm thick, a line 2 μm wide is obtained.

The other version has an interchangeable optical system giving reduction of 10× or 4× and is used to

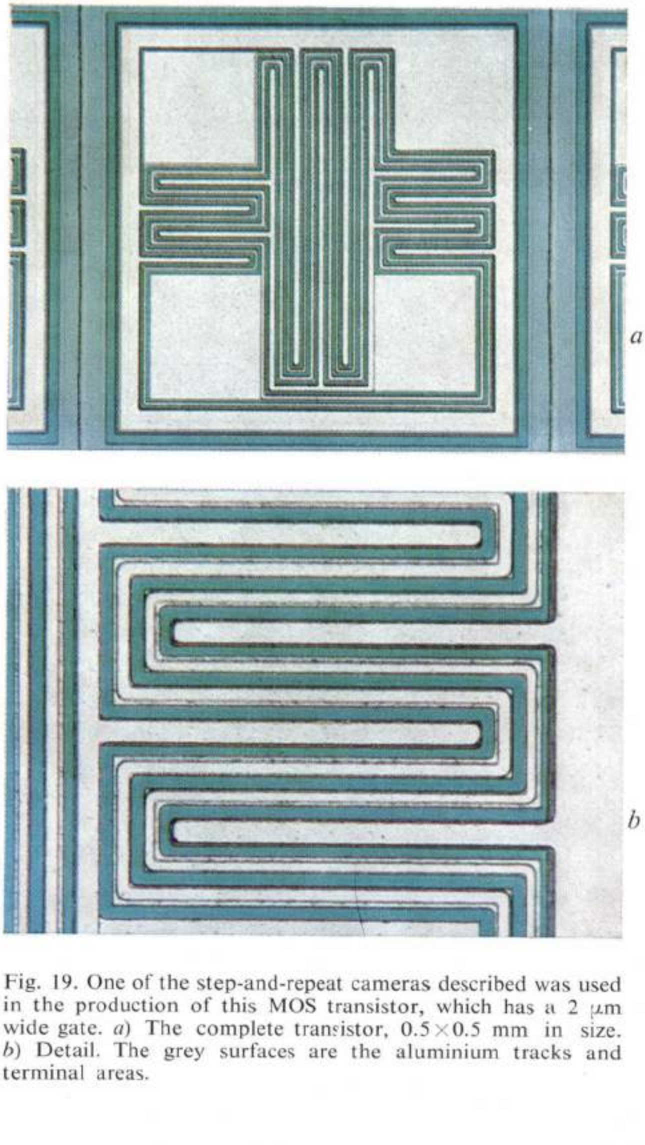

a

b

Fig. 19. One of the step-and-repeat cameras described was used in the production of this MOS transistor, which has a 2 μm wide gate. *a*) The complete transistor, 0.5×0.5 mm in size. *b*) Detail. The grey surfaces are the aluminium tracks and terminal areas.

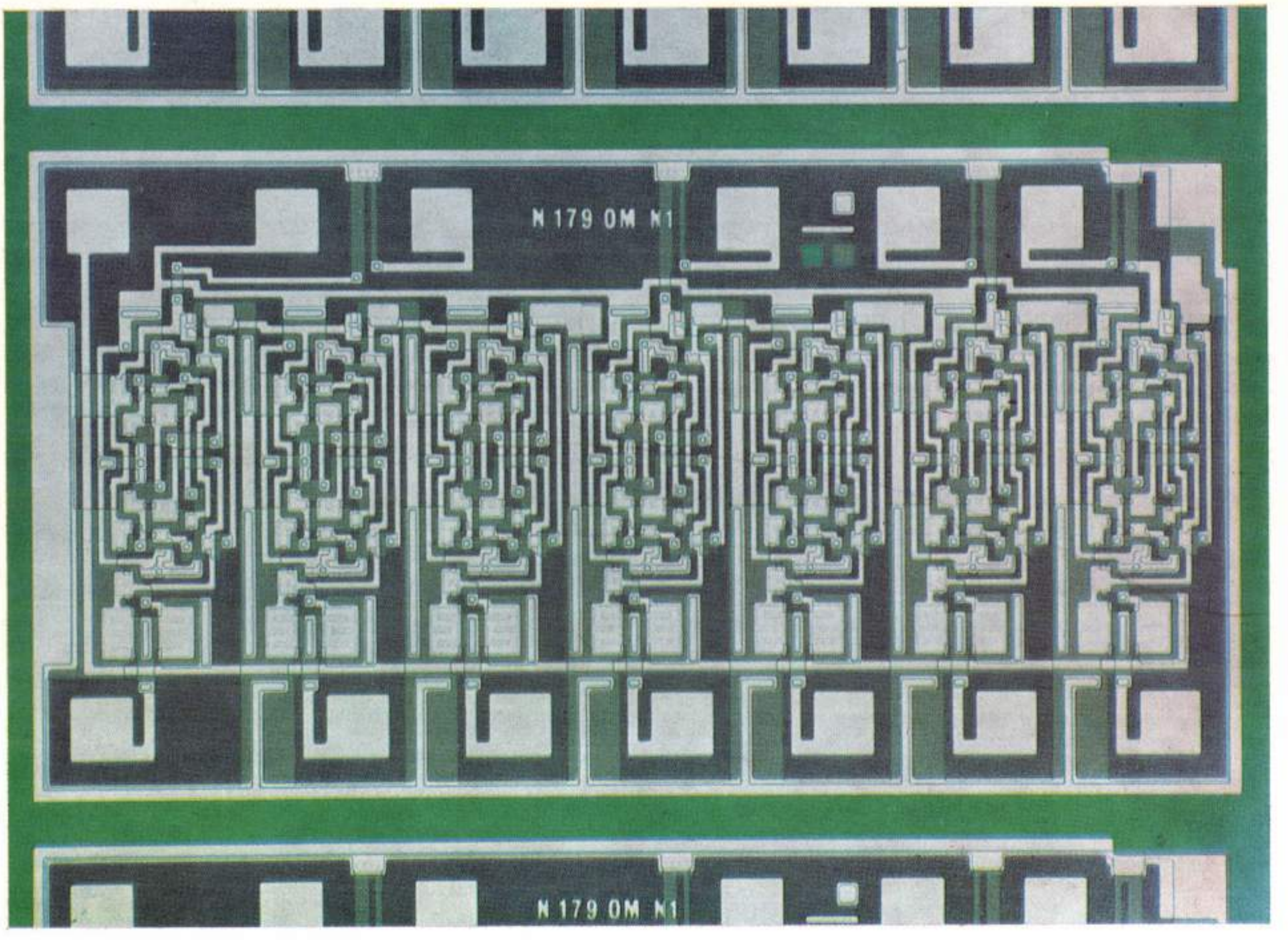

Fig. 20. A complete integrated circuit (a binary divider) made with the aid of one of the step-and-repeat cameras described. Dimensions 2.0 × 1.08 mm.

make photomasks for larger integrated circuits. Lines with widths of 2 and 3 μm in fields with diameters of 4.3 and 10 mm respectively can be obtained. *Fig. 20* shows an example of a larger integrated circuit produced with the aid of this camera.

The development of the step-and-repeat camera described here was made possible by the cooperation of many members of these Laboratories and of the Electronic Components and Materials Division (Elcoma). In particular the contribution made by A. G. Bouwer of the Precision Engineering Group of these Laboratories should be mentioned.

Summary. The photographic process used in the production of integrated circuits requires a set of photomasks that register very accurately with each other. These are made by photographic reduction of mask patterns; in this process 100 to 10 000 single images of the pattern for a circuit, each typically 1 × 1 mm, are formed on one mask for the purposes of quantity production. One method now widely used for making the masks employs a step-and-repeat camera, in a multi-barrel arrangement, for producing several masks simultaneously. The article describes a six-barrel step-and-repeat camera with carriages moving on hydrostatic bearings and a new grating measuring system for controlling their movements. As a result of numerous refinements in the bearings, in the measurement of displacement and in the adjustment of the object plates with the mask patterns and the focusing of the objectives, together with close control of the temperature, the total "repetition error", i.e. the relative error between two masks when one is placed on top of the other (whether produced simultaneously or successively), has been kept down to ± 0.2 micron. Various examples are shown.